

Recurrence properties of quantum observables in wave packet dynamics

C. Sudheesh*

Department of Mathematics, Indian Institute of Science, Bangalore 560 012, India

S. Lakshmibala[†] and V. Balakrishnan[‡]

Department of Physics, Indian Institute of Technology Madras, Chennai 600 036, India

(Dated: April 6, 2019)

We investigate the recurrence properties of the time series of quantum mechanical expectation values, in terms of two representative models for a single-mode radiation field interacting with a nonlinear medium. From recurrence-time distributions, return maps and recurrence plots, we conclude that the dynamics of appropriate observables pertaining to the field can vary from quasiperiodicity to hyperbolicity, depending on the extent of the nonlinearity and of the departure from coherence of the initial state of the field. We establish that, in a simple bipartite model in which the field is effectively an open quantum system, a decaying exponential recurrence-time distribution, characteristic of a hyperbolic dynamical system, is associated with chaotic temporal evolution as characterized by a positive Liapunov exponent.

PACS numbers: 05.45.Tp, 05.45.Mt, 42.50.Ar, 42.50.Dv, 42.50.Md

I. INTRODUCTION

Poincaré recurrences of classical dynamical systems yield a great deal of information on their ergodicity properties[1]. Recurrence-time statistics complements and augments the information obtained from other well-known signatures and quantifiers of dynamical behavior such as return maps, Liapunov spectra, time-series analysis, generalized dimensions, and so on.

There exists a body of rigorous results in the theory of dynamical systems that pertains to universal properties of recurrences. Most notably, for Axiom-A systems[2, 3, 4] and more generally for uniformly hyperbolic systems[5], the recurrence time to a sufficiently small cell in phase space is exponentially distributed. Moreover, successive recurrence times are independently distributed, so that the sequence of these recurrence times has a Poisson limit law. These are familiar features of stochastic systems (e. g., aperiodic Markov chains[6, 7, 8]), but the significant point is that they are also exhibited by deterministic systems with a sufficient degree of mixing. More detailed studies of recurrence-time statistics have been carried out in the case of low-dimensional chaotic systems, in particular, in the framework of one-dimensional maps. These investigations enable us to distinguish clearly between different degrees of randomness in the dynamics, ranging from quasiperiodicity through intermittency to fully-developed chaos[9, 10]. Departures from the standard results for hyperbolic systems have been analyzed, showing (for instance) that intermittency leads to power-law (as opposed to exponential) distributions of recurrence times, with cor-

relations between successive recurrences[11] and non-Poisson limit laws[12]. A variety of results is also known for recurrence-time distributions for Hamiltonian systems and for measure-preserving maps that model aspects of such systems. Interesting universal asymptotic properties, including power-law distributions of recurrence times, can arise here owing to the highly non-uniform nature of the invariant sets in phase space and the stickiness associated with the remnants of invariant tori[13, 14, 15, 16, 17, 18, 19, 20].

Besides recurrence-time distributions, recurrence plots comprise a related technique for analyzing dynamics ranging from periodicity to chaos[21, 22]. Several distinctive features of recurrence plots have been identified and established as indicators of specific kinds of dynamical behavior such as multiple periodicity, intermittency, and chaos. Recurrence quantification analysis[23] has been developed in an attempt to deduce quantitative information from the heuristics of recurrence plots.

In contrast to these detailed results for classical dynamical systems, the ergodicity properties of expectation values of observables in nonlinear quantum systems, regarded as dynamical variables, are much less comprehensively understood. A fundamental difficulty that immediately arises here is that the ‘phase space’ is effectively infinite-dimensional, because the complete information contained in a specific quantum state can be obtained, in principle, only if the mean values as well as all the higher moments and cross-correlators of all the quantum operators pertaining to the system are included in the set of dynamical variables. Moreover, significant roles are played by the precise nature of the initial state of the system, and by the interaction of the system of interest with the environment. Owing to these factors (and, of course, the non-commutativity of different operators), the dynamics of expectation values may be expected to be quite complex, even in relatively simple systems. It is therefore relevant to examine specific tractable models

*Electronic address: sudheesh@math.iisc.ernet.in

[†]Electronic address: slbala@physics.iitm.ac.in

[‡]Electronic address: vbalki@physics.iitm.ac.in

of quantum dynamics in order to disentangle the effects of various factors, and to discern systematic trends.

The time evolution of quantum mechanical wave packets provides an appropriate framework for the purposes described above. The phenomenon of revivals[24] provides a manifest analog of recurrences in coarse-grained dynamical systems. An initial state $|\psi(0)\rangle$ has a revival time T_{rev} if the overlap function $|\langle\psi(0)|\psi(T_{\text{rev}})\rangle|^2$ returns to an ϵ -neighborhood of its initial value of unity. A physical realization of this phenomenon is provided by the propagation of a radiation field in a nonlinear medium under suitable conditions. A wave packet of the radiation spreads and loses its original form almost immediately owing to the field-atom interaction, but displays revivals at integer multiples of T_{rev} . Correspondingly, all expectation values return to the neighborhoods of their initial values. Distinctive signatures of the revivals, and of the fractional revivals in between successive revivals, can be identified by analyzing the (projections of the) ‘phase trajectories’ of the system in subspaces of appropriate expectation values[25]. Typically, the behavior of these trajectories is similar to that of the phase trajectories in quasiperiodic dynamical systems with many incommensurate frequencies.

However, departures from this scenario occur with increasing deviation of the initial state from perfect coherence, or increasing nonlinearity of the medium, or both: It is found[26] that regular revivals of wave packets no longer occur under these conditions, namely, high nonlinearity and non-coherent initial states. A more detailed examination of this physically interesting, and obviously more generic, regime is called for. This is the primary objective of the present paper. The objects we study are the time series formed by the expectation values of relevant operators. The aspects we focus on are the recurrence-time or first-return-time statistics of these time series, and their recurrence plots.

In what follows, we use two simple models that capture the essence of the effects we seek to clarify and highlight. In the first of these, considered in Sec. II, we use the fact[27] that certain aspects of the dynamics of the radiation field propagating in a nonlinear medium can be modeled by an effective Hamiltonian involving the field operators alone, without explicitly invoking the atomic operators. The purpose here is to understand the effects of the lack of coherence of the initial state of the wave packet upon its subsequent evolution and upon recurrence-time distributions. The Hamiltonian concerned has a purely discrete spectrum, which implies, according to a rigorous result[28], that the dynamics of expectation values cannot be chaotic (the maximal Liapunov exponent cannot be positive). Nevertheless, we find that, with increasing nonlinearity and/or lack of coherence in the initial state, the recurrence-time distribution of a generic observable changes from a form that is characteristic of quasiperiodicity to an exponential distribution, which is customarily associated with hyperbolic (and hence chaotic) motion in classical dynamics. An exponential recurrence-time dis-

tribution is therefore not restricted to chaotic systems.

While this model serves to illustrate the point just made, it must however be recognized that the radiation field is really one of the two components of a bipartite, interacting, field-atom system. In order to investigate what happens in this situation, we consider, in Sec. III, a bipartite Hamiltonian that involves both the field operators and the atomic ladder operators. Focusing on operators involving the field mode alone then amounts, effectively, to considering an *open* quantum system interacting with the (atomic) environment. Even if the initial state is a non-entangled direct product state of the two modes, entanglement sets in during temporal evolution. The controlling parameter in this case is the ratio of the respective strengths of the nonlinearity and the intermode coupling. For low values of this ratio, an entangled state periodically factorizes into the initial product state (apart from an overall phase), and revivals occur. For higher values of the ratio, such revivals disappear. Depending on how far the initial state of the field is from perfect coherence, the dynamics of relevant expectation values emulates that of a hyperbolic dynamical system. Recurrence-time distributions, recurrence plots, as well as a calculation of the maximal Liapunov exponent based on phase-space reconstruction using the time series of an expectation value, all corroborate this conclusion, which therefore has implications for the dynamical behavior of open quantum systems.

II. SINGLE-MODE NONLINEAR HAMILTONIAN

As stated in the Introduction, we begin with a simple effective Hamiltonian for a single-mode electromagnetic field interacting with the atoms of a nonlinear medium,

$$H = \hbar(\chi a^{\dagger 2} a^2 + \chi' a^{\dagger 3} a^3), \quad (1)$$

where the photon annihilation and creation operators satisfy $[a, a^{\dagger}] = 1$. The first term in H is the standard one modeling a Kerr medium, with a coupling strength χ . The second term is an additional cubic nonlinearity with a strength χ' . It introduces a second natural frequency into the system. Since χ'/χ is arbitrary and generically not a rational number, it modifies the relatively simple behavior in the absence of such a term. Both terms are of course diagonal in the number operator $a^{\dagger}a$, since $a^{\dagger 2}a^2 = a^{\dagger}a(a^{\dagger}a - 1)$ and $a^{\dagger 3}a^3 = a^{\dagger}a(a^{\dagger}a - 1)(a^{\dagger}a - 2)$. As a consequence, the mean photon number in any state of the system remains equal to its initial value as the state evolves in time.

We first recapitulate very briefly how revivals occur in the absence of the cubic nonlinearity, i.e., when $\chi' = 0$. At the instants $t = \pi/(k\chi)$ (where k is a positive integer), the time-evolution operator $U(t) = \exp(-iHt/\hbar)$, which is diagonal in the Fock basis, has matrix elements $\exp[-i\pi n(n-1)/k]$, where n denotes the eigenvalues of $a^{\dagger}a$. Even though the exponent here is quadratic rather

than linear in n , this exponential has interesting periodicity properties[29] as a function of n . As a consequence of these properties, $U(\pi/k\chi)$ can be expanded in a Fourier series with $\exp(-2\pi ij/k)$ as the basis functions, where the integer j runs over the range $1 \leq j \leq (k-1)$. If the initial wave packet is the Gaussian wave packet corresponding to a minimum-uncertainty coherent state (CS) $|\alpha\rangle$ (where $a|\alpha\rangle = \alpha|\alpha\rangle$ and $\alpha \in \mathbb{C}$), then the state at time $\pi/(k\chi)$ can be written as a finite linear combination of the states $|\alpha e^{-2\pi ij/k}\rangle$ (for odd k) or the states $|\alpha e^{i\pi/k} e^{-2\pi ij/k}\rangle$ (for even k). But these are again coherent states, with parameters that are just phase-shifted versions of the original parameter α . It is then easy to see that, at time $T_{\text{rev}} = \pi/\chi$ (corresponding to $k = 1$), the initial state revives for the first time. Periodic revivals occur at integer multiples of T_{rev} . Fractional revivals are also evinced at specific times in between successive revivals.

The time evolution is quite different when $\chi' \neq 0$. For generic initial wave packets and (irrational) values of the ratio χ'/χ , exact revivals do not occur. Correspondingly, in the space of observables, periodic returns of observables to their initial values is replaced by quasiperiodicity. Now, the dynamical behavior of expectation values in this model cannot become chaotic for any parameter values (as already mentioned), because the evolution is governed by a quantum Hamiltonian with a purely discrete spectrum[28]. However, as the mean photon number increases, or the initial state departs from perfect coherence, the quasiperiodicity involves an increasing number of incommensurate frequencies. Concomitantly, the recurrence-time distributions and recurrence plots go over from the forms characteristic of quasiperiodicity to those pertaining to a dynamical system with a much higher degree of mixing, as we shall see below.

Our aim is to examine the role played by the extent of coherence of the initial state on the recurrence properties. An obvious dynamical variable for this purpose is the expectation value of the quadrature $x = (a + a^\dagger)/\sqrt{2}$. The standard CS $|\alpha\rangle$ serves as the reference initial state of the field mode. The mean photon number in this state is of course $|\alpha|^2$, which we shall denote by ν . The non-coherent initial states we consider are photon-added coherent states (PACS)[30]. The normalized m -photon-added coherent state $|\alpha, m\rangle$ has a quantifiable (and, in principle, tunable) departure from perfect coherence and Poissonian photon statistics. It is defined as $|\alpha, m\rangle = (a^\dagger)^m |\alpha\rangle / [m! L_m(-\nu)]^{1/2}$, where m is a positive integer and L_m is the Laguerre polynomial of order m . The mean photon number in this state is given by $(m+1)[L_{m+1}(-\nu)/L_m(-\nu)] - 1$. Moreover, the variance of the photon number can be shown to increase sublinearly with the mean photon number, implying that the photon statistics is sub-Poissonian. With the experimental production and characterization of a 1-photon-added coherent state by quantum state tomography[31], photon-added coherent states are expected to play an increasingly significant role in future investigations.

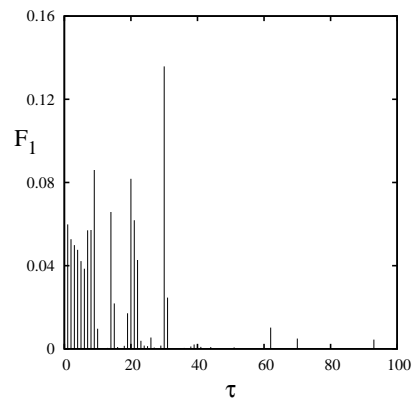


FIG. 1: First return time distribution F_1 of the expectation value $\langle x \rangle$. Initial state $|\alpha\rangle$, with $\nu = 1$.

The procedure we adopt is straightforward. We start with a given normalized initial state $|\psi(0)\rangle$, let it evolve unitarily according to the Hamiltonian H , and calculate $\langle \psi(t)|x|\psi(t)\rangle \equiv \langle x(t) \rangle$ in time steps δt . This produces a time series. The interval of values of $\langle x(t) \rangle$ is coarse-grained into small cells, and a recurrence to a given cell is marked. This enables us to build up the recurrence-time distribution for the cell concerned. The time series is also used to draw a recurrence plot. We have checked that the results reported below hold good qualitatively for generic cell sizes and locations in the phase space considered. For definiteness, we present in Figs. 1–6 the results for a cell size $\delta x = 10^{-2}$ and a parameter ratio $\chi'/\chi = 10^{-2}$. The data set comprises a long time series of about 10^7 points, and the time step $\delta t = 10^{-3}$. Time in units of δt is denoted by τ .

We now recall that, for uniform quasiperiodic motion with two incommensurate frequencies, the distribution of the time of recurrence to any cell (on the 2-torus) has a support comprising just three values[10, 32]. This result is derived from a ‘gap theorem’ for interval exchange transformations (specifically, the rotation map on a circle), and follows from certain number-theoretic properties of continued fractions[33, 34]. For quasiperiodic motion with more than two mutually incommensurate frequencies (i. e., on an n -torus with $n > 2$), the recurrence-time distribution remains a discrete distribution with support at a finite number of values (although no generally applicable formula is known for the actual number of such values, for arbitrary n). Returning to the problem at hand, we find that when the initial state is a CS $|\alpha\rangle$, with a mean photon number ν that is of the order of unity, the recurrence-time (or first return time) distribution F_1 of $\langle x \rangle$ is a discrete distribution with support at a small, finite number of points, as in Fig. 1. If, instead of the CS $|\alpha\rangle$, we use the PACS $|\alpha, m\rangle$ as the initial state, the points of support of the distribution F_1 increase in number with increasing m . Figure 2 illustrates the case $m = 5$. As m takes on larger values, this trend rapidly leads to an essentially continuous, decaying exponential

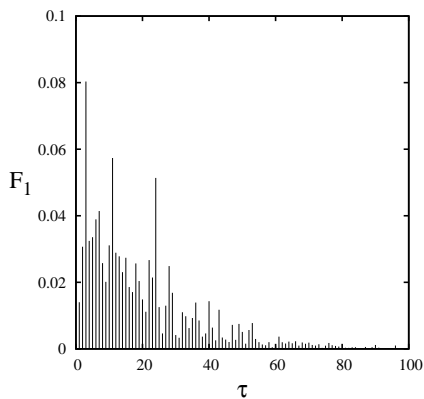


FIG. 2: F_1 for the initial state $|\alpha, 5\rangle$ with $\nu = 1$.

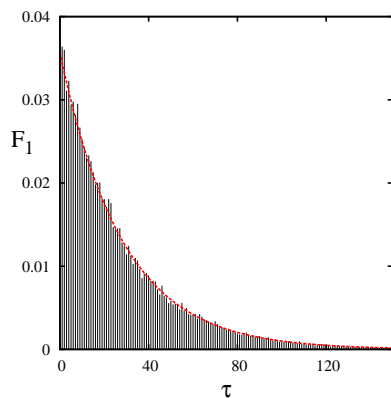


FIG. 3: F_1 for the initial state $|\alpha\rangle$ with $\nu = 100$.

distribution. The same trend occurs even for an initially coherent state $|\alpha\rangle$, provided the mean photon number $\nu \gg 1$, as seen in Fig. 3. The onset of an exponential distribution is even more pronounced for an initial PACS, as may be seen in Fig. 4.

The recurrence plots obtained from the time series for $\langle x \rangle$ are completely consistent with this scenario. Figure

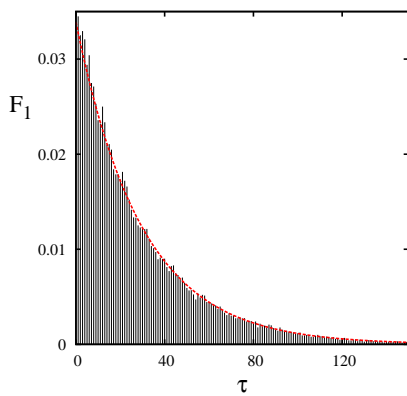


FIG. 4: F_1 for the initial state $|\alpha, 5\rangle$ with $\nu = 100$.

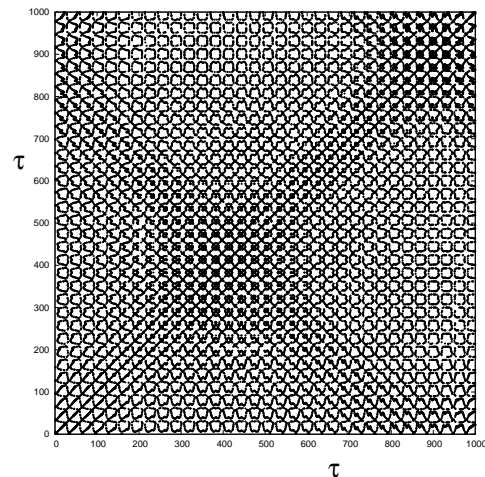


FIG. 5: Recurrence plot of the time series $\langle x \rangle$. Initial state $|\alpha\rangle$ with $\nu = 1$.

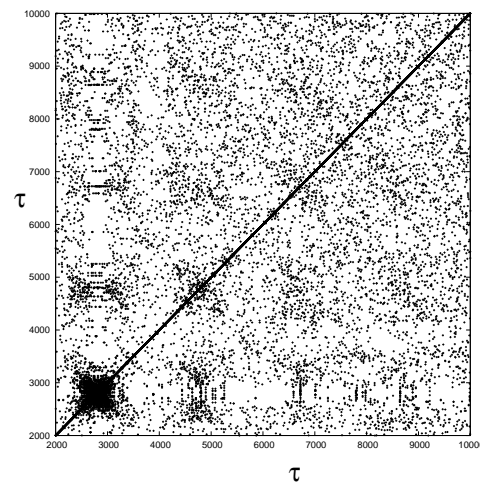


FIG. 6: Recurrence plot of the time series of $\langle x \rangle$. Initial state $|\alpha, 5\rangle$ with $\nu = 100$.

5 depicts the recurrence plot in the case of an initial CS $|\alpha\rangle$ with $\nu = 1$. The regular, patterned structure of the plot is characteristic[22] of quasiperiodicity with a relatively small number of incommensurate frequencies. In marked contrast, Fig. 6 shows the recurrence plot for an initial PACS $|\alpha, 5\rangle$ with $\nu = 100$. It is evident that, at the very least, a significant degree of mixing has set in, corroborating what we have already deduced on the basis of the recurrence-time distributions.

We are thus led to the conclusion that the generic dynamics in this model makes a gradual transition from quasiperiodicity to mixing as the mean photon number increases, *or* if the initial state deviates significantly from perfect coherence, *or* both. It has already been mentioned that hyperbolically unstable dynamics is precluded in this model. We have checked this out independently by augmenting the foregoing with an analysis of the time series obtained for $\langle x \rangle$ along the lines

customary[35, 36, 37] in the study of dynamical systems, namely: phase space reconstruction, the estimation of the minimum embedding dimension of the effective phase space, and the calculation of the maximal Lyapunov exponent λ_{\max} . The result, as expected, is that $\lambda_{\max} = 0$ to within numerical accuracy. The occurrence of an exponential recurrence-time distribution is not inconsistent with this result. As is familiar from results for Markov processes, exponential recurrence-time distributions and statistically independent successive recurrences with a Poisson law can occur even in stable stochastic dynamics[38] with a (mean) maximal Lyapunov exponent[39] that is zero or negative. The essential requirement is an adequate degree of mixing.

III. TWO-MODE MODEL: OPEN QUANTUM SYSTEM

Having seen how the introduction of the cubic nonlinearity in the single-mode model of Sec. II alters its dynamical behavior, we now turn to a more representative model of the radiation field propagating in a nonlinear medium. This model involves both the field and atom modes explicitly, and is given by the bipartite Hamiltonian[40]

$$H = \hbar[\omega a^\dagger a + \omega_0 b^\dagger b + \gamma b^{\dagger 2} b^2 + g(a^\dagger b + b^\dagger a)]. \quad (2)$$

As before, a and a^\dagger are the annihilation and creation operators for the field. The medium is modeled by an anharmonic oscillator with ladder operators b and b^\dagger , the parameter γ serving as a measure of the nonlinearity. We focus on the relative roles of the nonlinearity and the coupling of the two modes (quantified by the coupling constant g) in determining the dynamics of observables. In the numerical results presented below, we have therefore set the unperturbed frequencies ω and ω_0 equal to unity. The relevant tunable parameter is then the ratio γ/g . The idea is to examine the expectation value of an operator pertaining to the field alone, which may be regarded as an open quantum system in interaction with the ‘environment’ represented by the medium. Since an open subsystem of a Hamiltonian system is not conservative by itself, its evolution is effectively guided by a positive map, and any hyperbolicity in the dynamics could also lead to chaotic behavior of the observable concerned.

The total number operator $(a^\dagger a + b^\dagger b)$ commutes with the Hamiltonian (2) for all values of the parameters in H , but the photon number operator $a^\dagger a$ does not do so for any $g \neq 0$. Thus, while H can be cast in block-diagonal form in a direct-product basis of field and atom Fock states, the model is not trivial. The Fock basis is given by $|n\rangle_{\text{field}} \otimes |n'\rangle_{\text{atom}}$, where n and n' are the eigenvalues of $a^\dagger a$ and $b^\dagger b$ respectively. The basis states can be conveniently taken to be $|N - n\rangle_{\text{field}} \otimes |n\rangle_{\text{atom}} \equiv |N - n; n\rangle$, where N labels the eigenvalues of $(a^\dagger a + b^\dagger b)$. But $\langle N - n; n | H | N' - n'; n' \rangle = 0$ if $N \neq N'$. Hence, for a given value of N , H can be diagonalized in the space of

states $|N - n; n\rangle$, where $n = 0, 1, \dots, N$. A natural choice for the observable representing the field (the ‘open’ subsystem) is the photon number operator $a^\dagger a$.

It is evident that if $g = 0$, H is just the sum of two decoupled parts. If $\gamma = 0$, H is linear and hence is again trivially diagonalizable, and there is periodic exchange of energy between the field and the atomic oscillator. When γ and g are both non-zero, the dynamics is more complicated, but the existence of the conserved operator $(a^\dagger a + b^\dagger b)$ ensures that the system as a whole is well-behaved, with a discrete spectrum labeled by the quantum numbers N and s , where $N = 0, 1, \dots$ and $s = 0, 1, \dots, N$. The time-dependence of $\langle a^\dagger a \rangle$ is thus a direct consequence of the coupling of the field mode to another degree of freedom; and the deviation of $\langle a^\dagger a \rangle$ from periodic temporal variation is an indicator of the effects of the nonlinearity in the second degree of freedom. For different ranges of values of the parameter ratio γ/g , a diversity of temporal behavior is exhibited by $\langle a^\dagger a \rangle$. In the weakly nonlinear case ($\gamma/g \ll 1$), collapses and revivals of $\langle a^\dagger a \rangle$ occur almost periodically in time for initial field states which are Fock states or coherent states. When $\gamma/g \sim 1$, such collapses and revivals occur more irregularly if the field is initially in a coherent state, as compared to an initial Fock state. In the strongly nonlinear regime ($\gamma/g \gg 1$), collapses and revivals do not occur, and the model exhibits more complex dynamical behavior[26]. Our interest here is in the recurrence properties of the field observable $\langle a^\dagger a \rangle$. For illustrative convenience, we take the atomic oscillator to be in the ground state and the initial state of the field to be either a CS or a PACS. We shall denote the corresponding states of the total system by $|\alpha; 0\rangle$ and $|(\alpha, m); 0\rangle$, respectively.

In the case of weak nonlinearity, the return maps, recurrence plots, and first return distributions indicate quasiperiodicity of the field observables, remaining qualitatively independent of whether the initial state of the field is a CS or a PACS, and of the location and size of the cell in the coarse-grained ‘phase space’ (i. e., the bin in $\langle a^\dagger a \rangle$). These results are consistent with the occurrence of revivals, and hence of returns of observables to their initial values. Figures 7–10 correspond to an initial state $|\alpha; 0\rangle$, with $\nu = 1$ and $\gamma/g = 10^{-2}$. The return map in Fig. 7 and the recurrence plot in Fig. 8 reveal regular structures, while the distribution of the first return time for a typical cell is a sparse set of spikes. Figure 9 depicts F_1 for the cell C defined by the range $[0.596, 0.604]$ of $\langle a^\dagger a \rangle$. All these features are characteristic of quasiperiodic dynamics. A numerical evaluation of the (invariant) density ρ of $\langle a^\dagger a \rangle$, the results of which are depicted in Fig. 10, shows that this quantity is essentially made up of a large number of spikes.

For strong nonlinearity ($\gamma/g \gg 1$), however, revivals do not occur for generic conditions, and there arises a range of ergodicity properties, depending on the extent of coherence of the initial state of the field. For a significant departure from coherence (as measured by the ratio m/ν for an initial PACS), or even for sufficiently large values

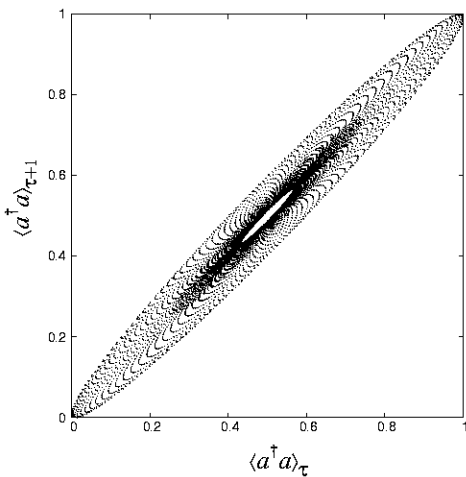


FIG. 7: Return map of the mean photon number $\langle a^\dagger a \rangle$ for an initial state $|\alpha; 0\rangle$ with $\nu = 1$; $\gamma/g = 10^{-2}$.

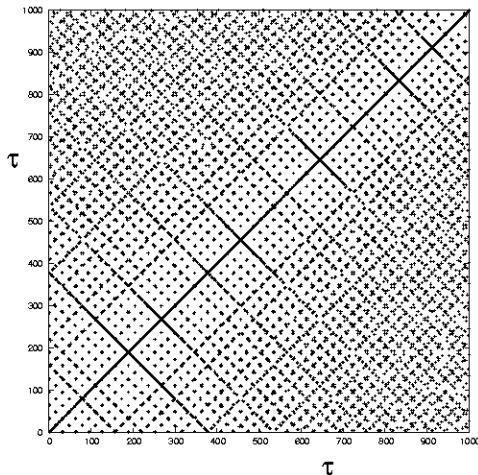


FIG. 8: Recurrence plot of $\langle a^\dagger a \rangle$ for the initial state $|\alpha; 0\rangle$ with $\nu = 1$; $\gamma/g = 10^{-2}$.

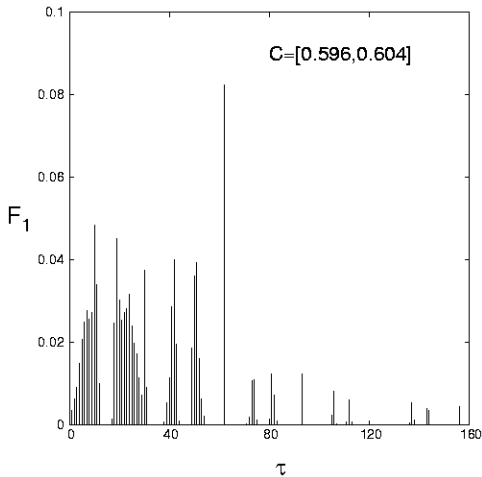


FIG. 9: First return time distribution F_1 of $\langle a^\dagger a \rangle$ to the cell C , for the initial state $|\alpha; 0\rangle$ with $\nu = 1$; $\gamma/g = 10^{-2}$.

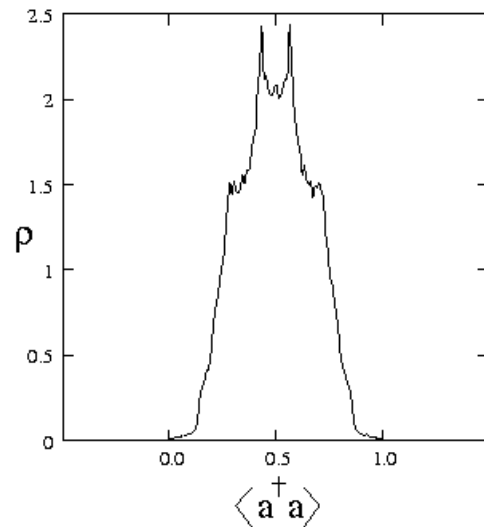


FIG. 10: Invariant density of $\langle a^\dagger a \rangle$. Initial state $|\alpha; 0\rangle$ with $\nu = 1$; $\gamma/g = 10^{-2}$.

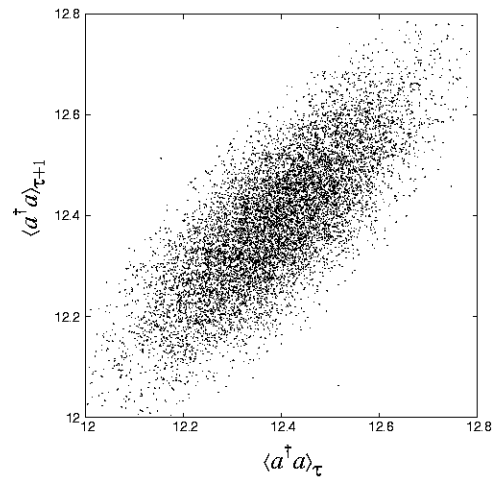


FIG. 11: Return map of the mean photon number $\langle a^\dagger a \rangle$ for the initial state $|(\alpha, 5); 0\rangle$ with $\nu = 5$; $\gamma/g = 5$.

of ν in the case of an initial CS, the dynamics of $\langle a^\dagger a \rangle$ effectively becomes hyperbolic. The return map and recurrence time statistics reveal this feature: the corresponding plots are in sharp contrast to those that arise in the quasiperiodic case. We illustrate this by means of plots for an initial state $|(\alpha, 5); 0\rangle$, with $\nu = 5$ and $\gamma/g = 5$. The return map (Fig. 11) and the recurrence plot (Fig. 12) no longer have well-defined patterns. The first return time distribution to a cell $C = [12.455, 12.465]$, shown in Fig. 13, approaches an exponential distribution (dotted lines), while the invariant density of $\langle a^\dagger a \rangle$, depicted in Fig. 14, is consistent with a continuous distribution.

As in the case of the single-mode model of Sec. II, the analysis of recurrence time distributions and recurrence plots is supplemented by a time series analysis leading to the estimation of the minimum embedding dimension

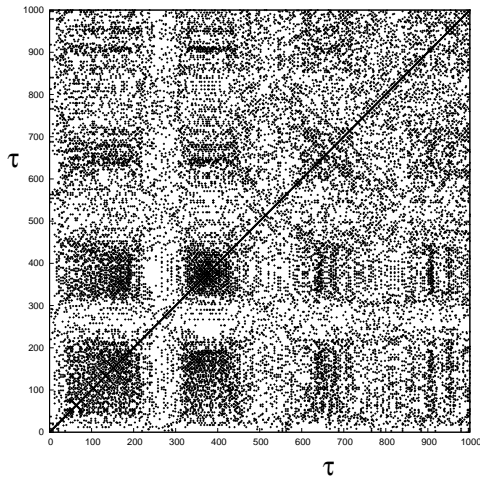


FIG. 12: Recurrence plot of $\langle a^\dagger a \rangle$ for the initial state $|(\alpha, 5); 0\rangle$ with $\nu = 5$; $\gamma/g = 5$.

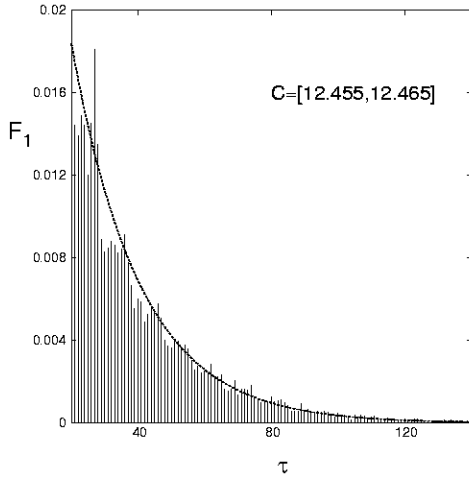


FIG. 13: First return distribution F_1 of $\langle a^\dagger a \rangle$ for the initial state $|(\alpha, 5); 0\rangle$ with $\nu = 5$; $\gamma/g = 5$.

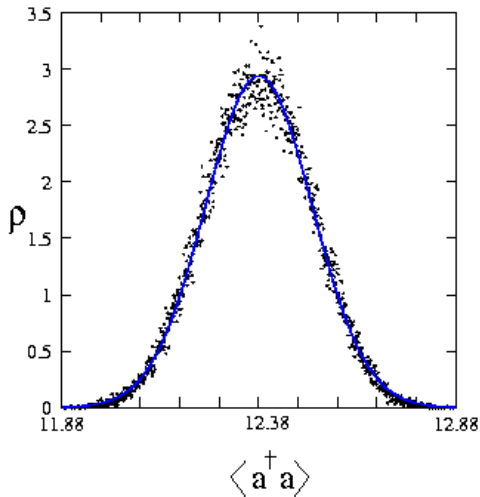


FIG. 14: Invariant density: Initial state $|(\alpha, 5); 0\rangle$ with $\nu = 5$; $\gamma/g = 5$.

		Increasing departure from coherence \rightarrow		
		Initial state		
		$ \alpha; 0\rangle$	$ (\alpha, 1); 0\rangle$	$ (\alpha, 5); 0\rangle$
Increasing nonlinearity \downarrow	$\gamma/g=10^{-2}$ $ \alpha ^2=\nu=1$	regular	regular	regular
	$\gamma/g=10^{-2}$ $\nu=5$	regular	regular	regular
	$\gamma/g=5$ $\nu=1$	regular	regular	chaotic exponential F_1 $\lambda_{\max} \approx 0.5$
	$\gamma/g=5$ $\nu=5$	chaotic exponential F_1 $\lambda_{\max} \approx 0.6$	chaotic exponential F_1 $\lambda_{\max} \approx 0.7$	chaotic exponential F_1 $\lambda_{\max} \approx 0.9$
	$\gamma/g=5$ $\nu=10$	chaotic exponential F_1 $\lambda_{\max} \approx 0.7$	chaotic exponential F_1 $\lambda_{\max} \approx 0.8$	chaotic exponential F_1 $\lambda_{\max} \approx 1.0$

TABLE I: Qualitative dynamical behavior of the mean photon number of a single-mode electromagnetic field interacting with a nonlinear medium.

and the calculation of the maximal Lyapunov exponent λ_{\max} . We have used [26] a robust algorithm developed by Rosenstein *et al.* [41] and Kantz [42] for the reliable estimation of λ_{\max} from data sets represented by time series. Table I gives a capsule summary of the representative results on the two-mode model of this Section. The characterizer ‘regular’ is used in those cases in which $\lambda_{\max} = 0$ to within numerical accuracy, while ‘chaotic’ indicates those corresponding to a positive value of λ_{\max} . It is immediately apparent that the latter is accompanied by an exponential recurrence-time distribution, in keeping with the known results for hyperbolic dynamical systems. As further corroboration we have also checked, in all these cases, that the distribution of two successive recurrences fits the next term in a Poisson distribution. The trends in the foregoing results are also in agreement with the results presented elsewhere [43] on the entanglement properties of the model, including, in particular, the behavior of the subsystem entropy corresponding to the field mode.

It is interesting that, even in as simple a model as the one considered here, where one of the components of a bipartite system effectively behaves like an open quantum system, the dynamical behavior can display such a range of ergodicity properties. The implications for genuine open quantum systems are therefore noteworthy.

-
- [1] M. Kac, *Probability and Related Topics in Physical Sciences*, (Interscience, 1959); Bull. Am. Math. Soc. **53**, 1002 (1947).
- [2] Y. Sinai, *Physica* **A163**, 197 (1970).
- [3] P. Collet, A. Galves, and B. Schmitt, Ann. Inst. H. Poincaré **57**, 319 (1992).
- [4] M. Hirata, *Ergod. Th. Dyn. Sys.* **13**, 533 (1993).
- [5] M. Hirata, in *Dynamical Systems and Chaos*, Vol. I, p. 87 (World Scientific, 1995).
- [6] W. Feller, *An Introduction to Probability Theory and Its Applications*, Vol. I (Wiley, 1962).
- [7] B. Pitskel, *Ergod. Th. Dyn. Sys.* **11**, 501 (1991).
- [8] D. R. Cox and H. D. Miller, *The Theory of Stochastic Processes* (Chapman and Hall, 1994).
- [9] V. Balakrishnan, G. Nicolis, and C. Nicolis, *J. Stat. Phys.* **86**, 191 (1997).
- [10] C. Nicolis, G. Nicolis, V. Balakrishnan, and M. Theunissen, in *Stochastic Dynamics*, Lecture Notes in Physics **484**, Eds. L. Schimansky-Geier and T. Pöschel (Springer Verlag, 1997).
- [11] V. Balakrishnan, G. Nicolis, and C. Nicolis, *Stochas. Dyn.* **1**, 345 (2001).
- [12] V. Balakrishnan and M. Theunissen, *Stochas. Dyn.* **1**, 339 (2001).
- [13] V. Afraimovich and G. M. Zaslavsky, in *Chaos, Kinetics and Nonlinear Dynamics in Fluids and Plasmas*, Lecture Notes in Physics **511** (Springer, 1998).
- [14] B. V. Chirikov and D. L. Shepelyansky, *Phys. Rev. Lett.* **82**, 528 (1999).
- [15] G. M. Zaslavsky and M. Edelman, *Chaos* **11**, 295 (2001).
- [16] N. Buric, A. Rampioni, G. Turchetti, and S. Vaienti, *J. Phys. A: Math. Gen.* **36**, L209 (2003).
- [17] N. Buric, A. Rampioni, and G. Turchetti, *Chaos, Solitons, Fractals* **23**, 1829 (2005).
- [18] E. G. Altmann and H. Kantz, *Phys. Rev. E* **71**, 056106 (2005).
- [19] E. G. Altmann, A. E. Motter, and H. Kantz, *Phys. Rev. E* **73**, 026207 (2006).
- [20] R. Artuso, L. Cavallasca, and G. Cristadoro, *Phys. Rev. E* **77**, 046206 (2008).
- [21] J.-P. Eckmann, S. O. Kamphorst, and D. Ruelle, *Europhys. Lett.* **4**, 973 (1987).
- [22] N. Marwan, M. C. Romana, M. Thiel, and J. Kurths, *Phys. Rep.* **438**, 237 (2007), and references therein.
- [23] N. Marwan, N. Wessel, U. Meyerfeldt, A. Schirdewan, and J. Kurths, *Phys. Rev. E* **66**, 026702 (2002).
- [24] R. W. Robinett, *Phys. Rep.* **392**, 1 (2004).
- [25] C. Sudheesh, S. Lakshmibala, and V. Balakrishnan, *Phys. Lett.A* **329**, 14 (2004); *Europhys. Lett.* **71**, 744 (2005).
- [26] C. Sudheesh, S. Lakshmibala, and V. Balakrishnan, *Phys. Lett. A* **373**, 2814 (2009).
- [27] R. Tanas, in *Theory of Nonclassical States of Light*, Editors V. V. Dodonov and V. I. Man'ko, (Taylor and Francis, 2003).
- [28] R. Kosloff and S. A. Rice, *J. Chem. Phys.* **74**, 1340 (1981).
- [29] I. Sh. Averbukh and N. F. Perelman, *Phys. Lett.A* **139**, 449 (1989).
- [30] G. S. Agarwal and K. Tara, *Phys. Rev. A* **43**, 492 (1991).
- [31] A. Zavatta, S. Viciani, and M. Bellini, *Phys. Rev. A* **72**, 023820 (2005).
- [32] S. Seshadri, S. Lakshmibala, and V. Balakrishnan, *Phys. Letters A* **256**, 15 (1999).
- [33] N. B. Slater, *Proc. Camb. Phil. Soc.* **63**, 1115 (1967).
- [34] G. Rauzy, *Acta Arith.* **34**, 315 (1979).
- [35] P. Grassberger and I. Procaccia, *Phys. Rev. Lett.* **50**, 346 (1983).
- [36] A. M. Fraser and H. L. Swinney, *Phys. Rev. A* **33**, 1134 (1986).
- [37] H. D. I. Abarbanel, *Analysis of Observed Chaotic Data*, (Springer, 1995).
- [38] V. Balakrishnan, G. Nicolis, and C. Nicolis, *Phys. Rev. E* **61**, 2490 (2000).
- [39] L. Arnold, *Stochastic Differential Equations: Theory and Applications* (Wiley, 1974).
- [40] G. S. Agarwal and R. R. Puri, *Phys. Rev. A* **39**, 2969 (1989).
- [41] M. T. Rosenstein, J. J. Collins, and C. J. D. Luca, *Physica D* **65**, 117 (1993).
- [42] H. Kantz, *Phys. Lett. A* **185**, 77 (1994).
- [43] C. Sudheesh, S. Lakshmibala, and V. Balakrishnan, *J. Phys. B: At. Mol. Opt. Phys.* **39**, 3345 (2006).